ELSEVIER

Journal of Photochemistry and Photobiology A: Chemistry 89 (1995) 221–227

Journal of PHOTOCHEMISTRY AND PHOTOBIOLOGY A: CHEMISTRY

Laboratory study of the respective roles of ferric oxide and released or added ferric ions in the photodegradation of oxalic acid in aerated liquid water

Chantal Guillard, Can fnm Hoang-Van, Pierre Pichat *, Frédérique Marme

URA au CNRS "Photocatalyse, Catalyse et Environnement", Ecole Centrale de Lyon, BP 163, F-69131 Ecully Cedex, France

Received 12 December 1994; accepted 16 February 1995

Abstract

These laboratory studies were aimed at distinguishing the relative importance of released or added ferric ions and of ferric oxide particles for the photodegradation of oxalic acid in natural waters. The parameters whose effects were determined for this purpose included the pH, the irradiation wavelength, the concentrations of the various species and the identity of the ferric oxide sample. In addition, the existence of a potential photocatalytic activity of ferric oxide was established by measurements of the electrical photoconductance of three samples under vacuum and in a dry dioxygen atmosphere. The results show the dominant role of ferric ions. However, the influence of ferric oxide is clearly not attributable to the mere dissolution. Effects due to the photoexcitation of surface iron–$HC_2O_4^-$ complexes are confirmed. Photocatalytic events may exist. The relative importance of these various phenomena depends on the $[Fe^{3+}]_{diss}/[Fe_2O_3]$ ratio and on the identity of the ferric oxide sample; in particular the crystallinity seems to favour the photodegradation of oxalic acid.

Keywords: Ferric oxide; Ferric ions; Oxalic acid; Natural waters; Atmospheric water; Photocatalysis; Photodegradation

1. Introduction

The Earth's crust contains about 5 wt.% iron, which is accordingly the fourth chemical element in order of importance. Ferric oxide, principally as haematite, is an abundant mineral. Natural waters contain both ferric oxide and iron ions. As a result of soil erosion and combustion of iron-containing materials, the amounts of ferric oxide and oxyhydroxides in the atmosphere are also important [1]; for example, they often represent between 5 and 15 wt.% of fly ashes [2]. These fine solid particles behave as condensation nuclei in the formation of fog and cloud water droplets in which iron ions dissolve. The amounts of iron ions in atmospheric water range from nanomoles per litre to millimoles per litre [3–6] and in other natural waters usually from tens to hundreds of micromoles per litre. These ions and ferric oxide play a role in the degradation of organic compounds and this study was carried out in this framework.

Ferric oxide electrodes have been used in photoelectrolysis cells [7] because of their sensitivity in the visible spectral region. Stable photocurrents were observed despite some dissolution, which, for a given electrode, depended on the electrolyte and increased with increasing radiant fluxes. Although the efficiency was obviously subordinate to the identity of the material, it remained low in all cases. Powdered haematite was found to be inactive for the oxidation of cyanide and active for that of sulphite and oxalate under UV irradiation [8]. Kormann et al. [9] have compared colloidal haematite with powdered ZnO and TiO_2 for oxidizing chlorinated organics in UV-irradiated aqueous suspensions. From their results and a critical review of literature data they concluded that ferric oxide was apparently "photocatalytically" active only in cases where the compound to oxidize was a strong reducing or complexing agent.

The photoredox reactions occurring in aqueous solutions containing oxalate and iron ions or iron oxides have recently been reviewed [10]. Hydrogenooxalate ions can be bound to the ferric oxide surface, forming several possible types of complexes in the inner coordination sphere. These complexes facilitate the reductive dissolution of ferric oxide. The detachment of the Fe^{2+} ions is easier for samples that are poorly crystallized. The inhibiting effect of dissolved dioxygen upon this detachment can be tentatively attributed to the trapping by this reactant of the electrons transferred from the valence band to the conduction band of the semiconductor photocatalyst by the irradiation. This phenomenon depends on the

* Corresponding author.

SSDI 1010-6030(95)04064-1

crystallinity. In solution hydroxyl radicals can be formed both from the photoexcitation of $Fe(OH)^{2+}$ and $Fe_2(OH)_2^{4+}$ entities [11] and from Fe(III) complexes with oxalate [12,13].

This study was undertaken as a supplementary attempt to assess the respective importances of dissolved ferric ions, surface organic complexes and the photocatalytic activity of ferric oxide in the degradation of oxalic acid. The practical goal was to gain a better understanding of the phenomena that may occur in atmospheric water droplets, in the photic zone of natural waters and on the surface of wet soils that principally contain ferric oxide. Oxalic acid was chosen because (i) it is found in atmospheric water droplets at concentrations similar to that of iron cations [13], (ii) it is a degradation product of many organic compounds and (iii) it readily forms complexes with ferric ions [14]. Our conclusions are based on studies of the effects of several parameters upon the photodegradation rate of oxalic acid. These parameters included the irradiation wavelength, the concentration of oxalic acid, the mass of ferric oxide or the concentration of ferric ions, the addition of ferric ions to suspensions of ferric oxide, the identity of the ferric oxide sample and the pH. Also, some measurements of the electrical photoconductance of three ferric oxide samples under vacuum or in a dry dioxygen atmosphere were carried out to gain information on the behaviour of light-irradiated ferric oxide in the absence of liquid water.

2. Experimental details

2.1. Materials and characterization techniques

Dehydrated oxalic acid (99%), $Fe_2(SO_4)_3 \cdot 5H_2O$ (97%) and $Fe(NO_3)_3 \cdot 9H_2O$ (99%) were purchased from Aldrich. Preparations and some characteristics of the ferric oxide samples are indicated in Table 1. The surface areas of these samples, evacuated at 423 K for 3 h, were measured by the Brunauer–Emmett–Teller (BET) method using dinitrogen. X-Ray diffraction patterns were recorded on a Siemens diffractometer using Co Kα radiation filtered through a nickel foil. Photoconductivity measurements were performed in a photoconductivity cell which was described previously [18].

2.2. Photoreactor and irradiation devices

The irradiation of the aqueous solutions or suspensions was carried out in a Pyrex cylindrical flask (total volume about 90 ml) with a bottom optical window whose surface area was approximately 11 cm^2 and which transmitted wavelengths greater than 290 nm. This flask was directly connected to a chromatograph to analyse the atmosphere above the liquid. In the case of the study of the influence of oxalic acid concentration, a flow of O_2 was bubbled in the solution before the irradiation was started. Two types of lamps were used. When a Philips HPK 125 W high pressure mercury lamp was employed, a circulating water cell 2.2 cm thick was placed in the incident beam to absorb the IR part of the emission. The radiant flux, measured with a power meter (United Detector Technology, model 21A) and entering the photoreactor, was 65 ± 2 mW cm^{-2}. To study the effect of various wavelengths, a xenon lamp (Hanovia 250 W) and interferential filters (365, 430, 576 and 675 nm) were used.

2.3. Procedures and analyses

Ten millilitres of oxalic acid solution was introduced into the photoreactor containing or not containing powder ferric oxide. The suspension was magnetically stirred for 30 min in the dark before it was irradiated. This period of time was sufficient to reach equilibrated dissolution of iron oxide and adsorption of oxalic acid. The kinetics of carbon dioxide evolution was monitored by use of an Intersmat IGC 120 MB gas chromatograph equipped with a Porapak Q column, 3 m

Table 1
Preparation methods and characteristics of the ferric oxide samples

Sample	Preparation method	Structure	Surface area ($m^2 g^{-1}$)	Iron ions dissolved [a] ($mmol l^{-1}$)	CO_2 [b] (%)
Fe_2O_3 Merck	Commercialized	Haematite	4	0.2	90
FeUR500	Decomposition of urea in presence of $(NH_4)_2SO_4$ and $Fe_2(SO_4)_3 \cdot 2H_2O$ at pH 2.2 [15,16]; calcination at 773 K	Amorphous	25	21	100
FeUR600	Same preparation as above, but calcination at 873 K	Haematite	23	1.25	52
FeNO120	Precipitation of $Fe(NO_3)_3$ by NH_4OH at pH 8 [17]; product then dried at 393 K in air	80% haematite, 20% goethite	181	0.036	48
FeNO500	Same preparation as above, but calcination at 773 K in flowing air	Haematite	19	0.053	82

[a] In the presence of 5 $mmol l^{-1}$ oxalic acid and air. Ferric oxide concentration: 10 $g l^{-1}$.
[b] The percentages relate to the total transformation of oxalic acid into CO_2. The values indicated are those corresponding to an irradiation of 80 min.

long and 6.3 mm inner diameter, and a catharometer. The absorbance spectra were determined at room temperature by use of a Perkin–Elmer Lambda 9 spectrophotometer. The concentrations of iron ions released by the ferric oxide samples (Table 1) and the pHs were measured by an ARL-Fison plasma ICP-AES and a Tacussel II ionoprocessor respectively.

3. Results and discussion

3.1. Assessment of the photocatalytic properties of Fe_2O_3

To assess the capability of ferric oxide to form electron–hole pairs when irradiated by photons of energy greater than the band gap, photoconductance measurements were carried out with the three samples Merck, FeUR500 and FeUR600 (Table 1). Fig. 1 shows the effect of switching on and off the UV irradiation under vacuum in the case of the Merck sample after a prolonged first irradiation necessary to reach equilibrium. These variations illustrate the photoexcitation of electrons to the conduction band of ferric oxide. The other two samples behaved similarly. When the evacuated, UV-irradiated samples were exposed to gaseous dioxygen, no variation in the photoconductance σ was observed for pressures below about 13.3 Pa. This means that at the corresponding surface coverages by oxygen species the rate of recombination of the photoproduced charges was much faster than the rate of capture of electrons by the oxygen species. Consequently, a poor photocatalytic activity for oxidation reactions can be predicted [18–20]. However, at higher dioxygen pressures $P(O_2)$, $\log \sigma$ was proportional to $\log[P(O_2)^{-0.5}]$, i.e. the electrical equilibrium was controlled by O^- species [18] at least up to the highest pressure used (667 Pa). This variation shows that, provided that the coverage of the ferric oxide surface by oxygen species is sufficient, some oxidative photocatalytic activity may ensue.

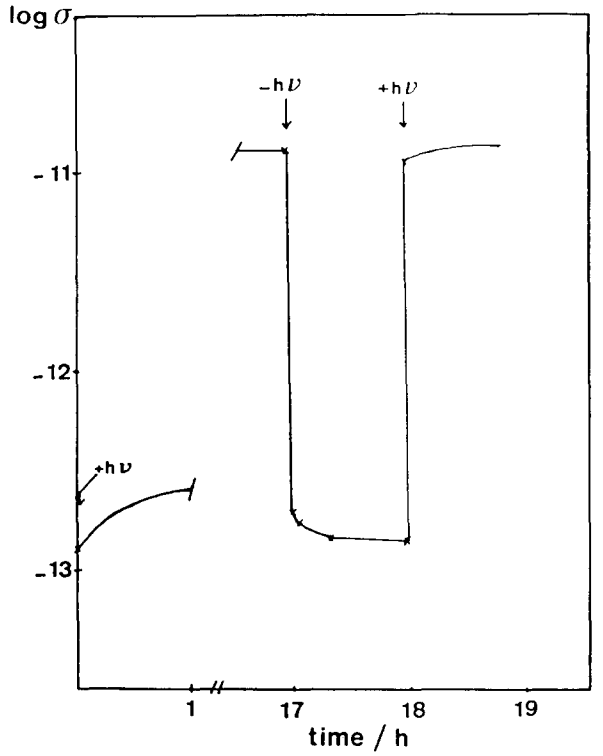

Fig. 1. Conductance σ (S) of Fe_2O_3 Merck under vacuum with and without irradiation at wavelengths greater than 220 nm. The variations shown here for one sequence can be repeated.

These experiments, performed with evacuated ferric oxide samples, are only indicative for the photodegradation of oxalic acid in aerated ferric oxide aqueous suspensions. In particular, the coordination of oxalate at the solid surface can change the photosensitivity. Nevertheless, previous studies [19,20] have shown correlations between the photoconductance variations and the photocatalytic activity for oxidations in various media.

3.2. Comparison between Fe_2O_3 and TiO_2

To demonstrate the importance of the effect of the combination of ferric oxide and the ferric ions released by this oxide upon the degradation of oxalic acid, we first compared this effect with that of titanium dioxide Degussa P-25, a semiconductor sample whose high photocatalytic activity is well known. Fig. 2 shows that these effects were very close when ferric oxide Merck was used. However, this does not mean that the photocatalytic activities of the two oxide samples were nearly equal, as was evidenced by replacing oxalic acid, which can bind to the surface of ferric oxide and form complexes with ferric ions [10], by acetaldehyde. The rate of formation of carbon dioxide from this latter pollutant was much faster in the presence of TiO_2 (Fig. 3). In other words, these comparisons already show that under our experimental conditions the photodegradation of oxalic acid is predominantly attributable to the existence of surface or dissolved iron–oxalate complexes and not to the photocatalytic activity of ferric oxide.

To further assess the relative importance of the two types of phenomena, we focused on the system oxalic acid/ferric oxide–ferric ions and varied several parameters.

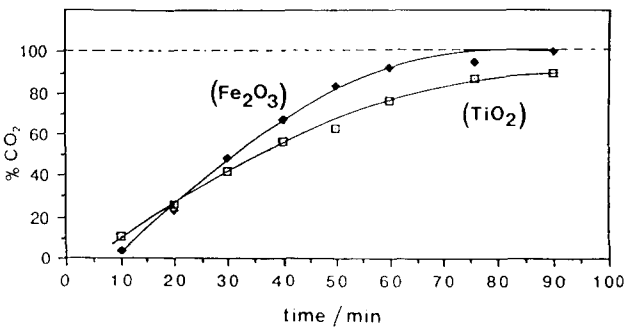

Fig. 2. Carbon dioxide formed from the photodegradation of oxalic acid (5 mmol l^{-1}, 10 ml, pH 2.3) as a function of irradiation time ($\lambda > 290$ nm) in the presence of TiO_2 P-25 Degussa (3.5 g l^{-1}) and haematite commercialized by Merck (2.0 g l^{-1}). The percentages relate to the total transformation of oxalic acid into CO_2.

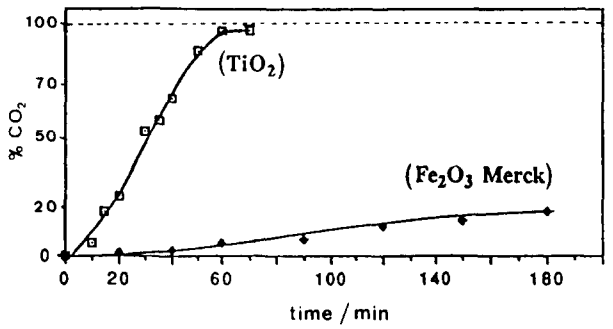

Fig. 3. Photodegradation of acetaldehyde (0.454 mmol l^{-1}, 20 ml). Other conditions as in Fig. 2, with the exception of the concentration of haematite (3.5 g l^{-1}).

3.3. Oxalic acid degradation at various wavelengths

The degradation of oxalic acid in the presence of ferric oxide was studied at various wavelengths by use of interferential filters to determine whether the action spectrum of the rate of carbon dioxide formation was similar to the absorption spectrum of the solid or of the solution containing ferric ions. The samples FeUR500 and Fe_2O_3 Merck were used (Table 1). Their concentration was 2 g l^{-1}, i.e. that corresponding to the maximum effect under polychromatic irradiation (see below). Fig. 4 shows that the action spectrum of the mean degradation rate of oxalic acid corresponded to the absorption spectrum of the solution (Fig. 4B) and not to that of the solid (Fig. 4A). Clearly, these results demonstrate that the formation of carbon dioxide from oxalic acid depended predominantly on the absorption of photons by iron–oxalate complexes. Nevertheless, they do not rule out the existence of a photocatalytic activity of the solid in so far as the two absorption spectra partly overlap below about 400 nm. The photochemical reductive dissolution of haematite in the presence of oxalate and in the absence of oxygen was also found to occur only at wavelengths shorter than about 400 nm [10b].

3.4. Rate–concentration relationships in the photodegradation of oxalic acid

Figs. 5 and 6 show the initial rate of CO_2 formation vs. the initial concentration C_o of oxalic acid in the presence of 0.2 mmol l^{-1} ferric ions, which corresponded to the concentration of iron ions released by the Merck sample in 5 mmol l^{-1} oxalic acid, and in the presence of the Merck sample respectively. The variations observed cannot be entirely attributed to the changes in initial pH from 3 to 1.3 approximately because of varying C_o (see Fig. 10 below), nor to increases in the release of iron ions from the Fe_2O_3 sample. The langmuirian form of the curve of Fig. 6 may be caused either by the photocatalytic activity of ferric oxide or by the formation of surface iron–oxalate complexes acting as the light-absorbing species. The linear transform of this curve (Fig. 6, inset) tends to show that oxalic acid was dissociatively adsorbed on ferric oxide.

The initial rate of carbon dioxide evolution, r_o, was higher in the presence of ferric ions alone, whatever C_o (Fig. 5). The proportionality of r_o to C_o suggests that iron–oxalate complexes caused the photodegradation. This proportionality was not observed for the highest C_o, presumably because of the absorption of uncomplexed oxalic acid.

These results show that ferric oxide played a role in the photodegradation of oxalic acid, although this role was markedly less important than that of ferric ions when these ions were present alone in the solution at a concentration of 0.2 mmol l^{-1}.

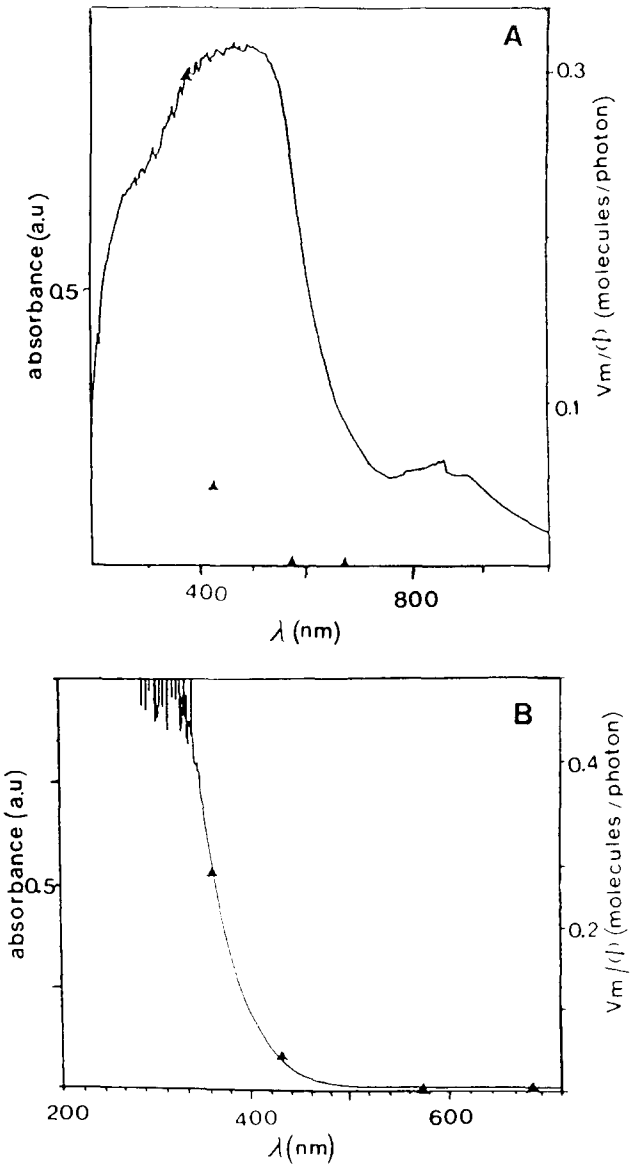

Fig. 4. Absorption spectra of (A) the FeUR500 sample (Table 1) and (B) the solution obtained by filtrating the suspension containing 2 g l^{-1} of this sample in 5 mmol l^{-1} oxalic acid, pH 2.3, which was stirred in the dark for 18 h. The triangles correspond to the mean rate v_m of CO_2 formation (resulting from the irradiation of the suspension at the indicated wavelengths for 70 h) divided by the radiant flux ϕ. Qualitatively similar results were obtained on replacing the FeUR500 sample by the Merck sample, but the v_m/ϕ ratios were smaller. Spectrum B is similar to that published in Ref. [13].

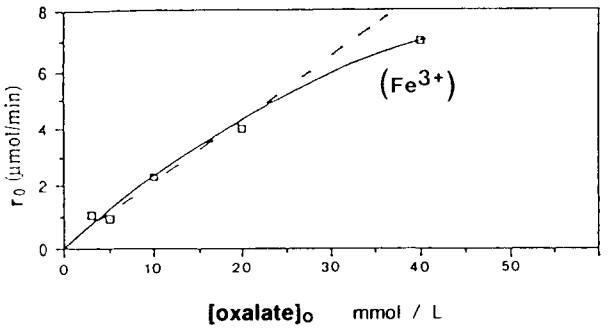

Fig. 5. Initial rate of formation of CO_2 as a function of the initial concentration of oxalic acid in the presence of 0.2 mmol l^{-1} ferric nitrate at $\lambda > 290$ nm (volume of suspension, 10 ml).

3.5. Oxalic acid photodegradation in the presence of various masses of Fe_2O_3 or concentrations of Fe^{3+} ions

Figs. 7 and 8 show the initial rate of formation of CO_2 from oxalic acid at $\lambda > 290$ nm in the presence of various concentrations of ferric ions and in the presence of various masses of two ferric oxide samples respectively.

Oxalic acid at the concentration of 5 mmol l^{-1} absorbs very weakly in this wavelength range and a control experiment showed that the evolution of CO_2 observed was not due to the direct photolysis. Moreover, the counter-ions did not play a role, since the effect of ferric nitrate or sulphate was the same.

The rate r_0 was proportional to $[Fe^{3+}]$ up to about 10 mmol l^{-1} (Fig. 7). This proportionality could be explained by the formation of iron–oxalate complexes which were photodegraded under irradiation. The decrease in r_0 beyond this concentration could arise either from an absorption competition between the ferric ions and the oxalate complexes or from the formation of polynuclear iron complexes which photodegrade less easily than the mononuclear complexes [21].

In the presence of the amorphous FeUR500 sample or the Merck haematite sample (Fig. 8) r_0 first increased with increasing masses of ferric oxide. The increase was more important with the FeUR500 sample which released more iron cations in the solution (Table 1). Because of the effect of ferric ions shown in Fig. 7, it is again inferred that carbon dioxide was predominantly formed by the photodegradation of iron–oxalate complexes. When concentrations of ferric oxide higher than about 20 g l^{-1} were employed, the role of the solid as an optical filter became dominant, which led to a decrease in r_0. This decrease cannot be attributed only to the absorption by ferric ions, because in that case the maximum of the two curves of Fig. 8 should not correspond to the same mass of ferric oxide for both samples. At the highest concentrations of ferric oxide the fact that r_0 was not zero could stem either from the photocatalytic activity of the oxide or from the photodegradation of surface iron–oxalate complexes.

3.6. Simultaneous effects of Fe_2O_3 and added $Fe(NO_3)_3$ on the photodegradation of oxalic acid

Fig. 9 shows the effect of adding ferric nitrate to a suspension containing 10 g l^{-1} of the haematite sample FeNO500 which released about 50 µmol l^{-1} iron ions (Table 1). Ferric ions at the concentration of 10 µmol l^{-1} without ferric oxide led to a very low photodegradation of oxalic acid (Fig. 9, curve (1)). Addition, to the suspension containing the FeNO500 sample, of 0.2 mmol l^{-1} of ferric ions, which was equivalent to the release of iron ions by the Merck haematite sample, did not change the photodegradation rate of oxalic acid (Fig. 9, curve (2)). Therefore it can be concluded that the formation of carbon dioxide was in that case due either to the photocatalytic activity of the FeNO500 sample or to the photoexcitation of surface iron–oxalate complexes. When the concentration of added ferric ions was 20 mmol l^{-1} (Fig. 9, curve (3)), the formation rate of CO_2 was increased and was equivalent to that observed without the solid (Fig. 9,

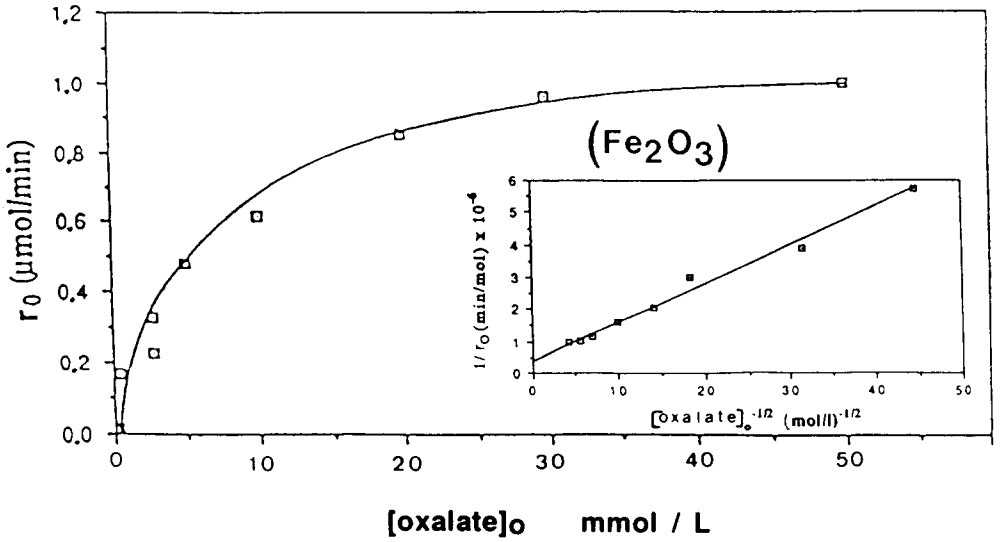

Fig. 6. As Fig. 5, but with ferric nitrate replaced by the Fe_2O_3 Merck sample (10 g l^{-1}). The inset shows the linear transform.

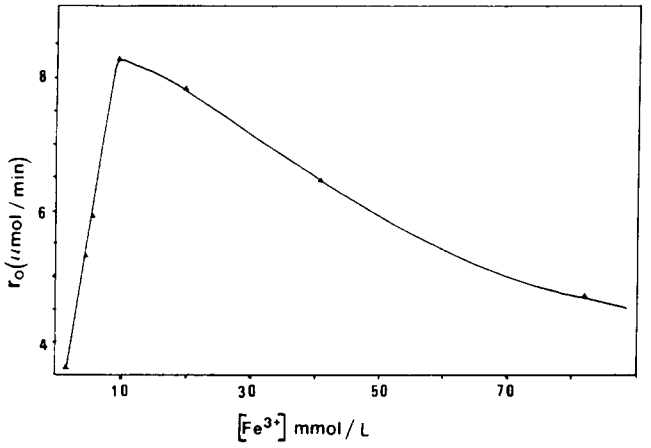

Fig. 7. Influence of the concentration of ferric ions (from ferric nitrate dissolved in 10 ml of distilled water) on the initial rate of photodegradation of oxalic acid (5 mmol l^{-1}, initial pH 2.3) at $\lambda > 290$ nm.

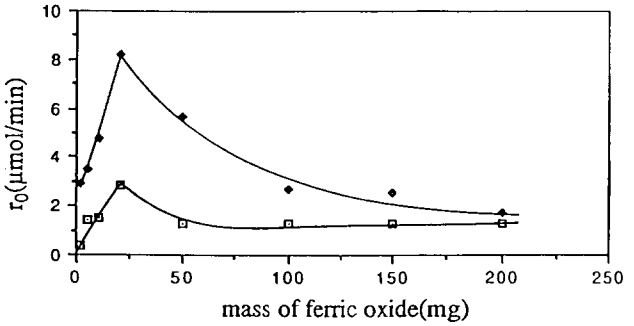

Fig. 8. Influence of the amount of ferric oxide (volume of suspension 10 ml) on the initial rate of photodegradation of oxalic acid (5 mmol l^{-1}, pH 2.3) at $\lambda > 290$ nm in the presence of the amorphous ferric oxide sample FeUR500 (diamonds) and the Merck sample (squares).

curve (4)). This high concentration was chosen because it corresponded to the release of iron ions by the FeUR500 sample (Table 1).

In conclusion, these experiments clearly show that the dominant origin of the photodegradation of oxalic acid depended upon the ratio $[Fe^{3+}]/[Fe_2O_3]$.

3.7. Effect of the identity of the ferric oxide sample on the photodegradation of oxalic acid

A series of ferric oxide samples were prepared and tested in the photodegradation of oxalic acid under identical conditions. Clearly, the dissolution of the samples (Table 1, fifth column) was not the only factor determining the evolution rate of carbon dioxide (Table 1, last column). This again emphasizes the role of the solid itself.

As various factors affected the surface properties, no really clear picture emerged concerning the importance of each factor. However, the comparison of two samples calcined at 393 and 773 K (FeNO120 and FeNO500 in Table 1) showed that the high temperature treatment, which completed the transformation of FeOOH (20% initially) into haematite, produced a sample giving rise to a higher rate of CO_2 evolution, despite a reduced surface area (19 $m^2\ g^{-1}$ instead of

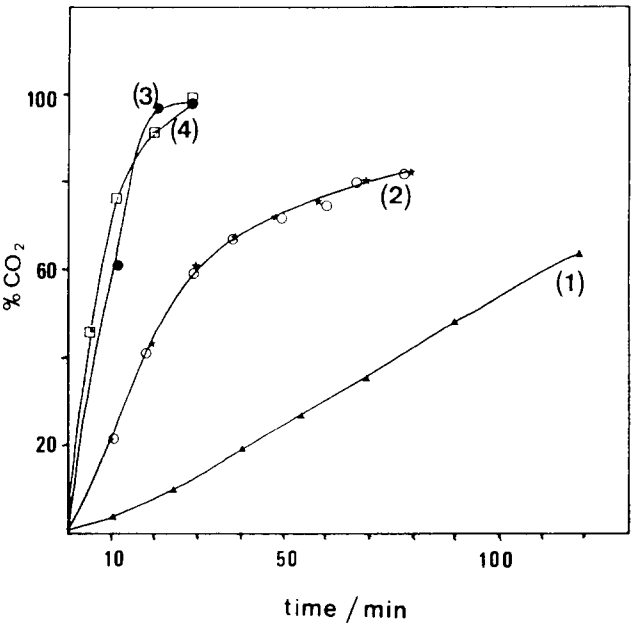

Fig. 9. Percentage of CO_2 formed by the photodegradation of oxalic acid (5 mmol l^{-1}, 10 ml, initial pH 2.3) at $\lambda > 290$ nm (100% corresponds to complete transformation) as a function of the irradiation time in the presence of (1) 10 µmol l^{-1} ferric nitrate, (2) 100 mg FeNO500 with (circles) and without (stars) 0.2 mmol l^{-1} ferric nitrate, (3) 100 mg FeNO500 and 20 mmol l^{-1} ferric nitrate and (4) 20 mmol l^{-1} ferric nitrate.

181 $m^2\ g^{-1}$), and equivalent small releases of iron ions. Therefore the increase in crystallinity was favourable for the photodegradation of oxalic acid.

Also, the comparison of two haematite samples (FeNO500 and FeUR600 in Table 1) with equivalent surface areas, prepared either from ferric nitrate or ferric sulphate, tends to show the unfavourable role of sulphate ions (see also Section 3.8), since the lowest rate of CO_2 evolution was observed with the ex-sulphate sample, although it released about 24 times more iron ions. Sulphate ions can be coordinated in the inner sphere of ferric oxide [15,22]. Accordingly, they modify the surface and can hinder the coordination of oxalate ions to the surface.

3.8. Effect of pH on the photodegradation of oxalic acid

The effect of pH on r_0 in the presence of Fe_2O_3 Merck and in the presence of ferric ions is shown in Fig. 10. Considering that the pK_A value of the couple $HC_2O_4^-/C_2O_4^{2-}$ is 4.19, it can be inferred from the smaller r_0 at pH 5 than at lower pHs that $HC_2O_4^-$ ions were involved in the formation of CO_2. A similar dependence on pH has been reported [13] for the formation of hydrogen peroxide from a sunlight-irradiated, aerated solution of ferric ions and oxalate.

The rate r_0 was identical whether $Fe(NO_3)_3$ or $Fe_2(SO_4)_3$ was used as the source of ferric ions and it also did not depend on whether HNO_3 or H_2SO_4 was added to reach pH 1.5. By contrast, the use of sulphuric acid in place of nitric acid decreased r_0 in the presence of the Fe_2O_3 Merck sample (Fig. 10). This influence can be attributed either to a competition

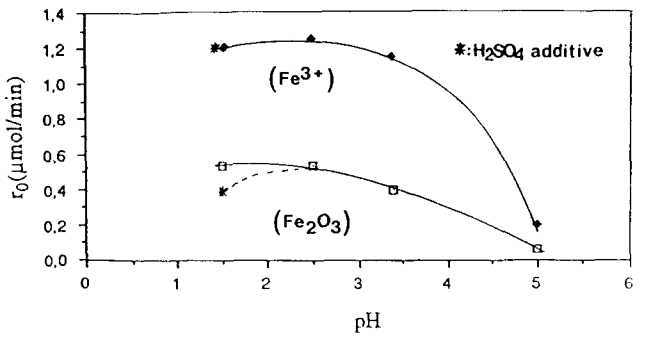

Fig. 10. Initial rate of formation of CO_2 from oxalic acid (5 mmol l^{-1}, 10 ml, $\lambda > 290$ nm) as a function of pH in the presence of Fe_2O_3 Merck (10 g l^{-1}) (squares) and ferric nitrate (0.2 mmol l^{-1}) (diamonds). The pH was adjusted with KOH (3.4 and 5) or with HNO_3 or H_2SO_4 (1.5).

between sulphate and oxalate for capturing the oxidizing species formed at the solid surface or, more likely, to a modification of the solid surface resulting from the location of sulphate ions in the inner coordination sphere [15,22]. Whatever the reason, the effect of sulphate also shows the involvement of the ferric oxide surface in the photodegradation of oxalic acid.

4. Conclusions

Since the photocatalytic activity of ferric oxide in the degradation of aqueous oxalic acid cannot be delineated from the photodegradation of iron–oxalate complexes either at the oxide surface or in the water bulk because of iron ion dissolution, we have tried to assess the importance of heterogeneous photocatalysis both from photoconductance measurements in the dry state and from comparisons with titanium dioxide in aqueous solutions. From these experiments it can be concluded that heterogeneous photocatalysis plays a minor role as compared with the other photoprocesses. This conclusion is also supported by the spectral sensitivity of the oxalic acid degradation. The role of the complexes formed at the solid surface [10] is confirmed and illustrated in particular by (i) the different patterns of the initial degradation rate against the initial concentration of oxalic acid in the presence of ferric ions or ferric oxide and (ii) the detrimental effect of sulphate ions used in the preparation of ferric oxide or added to the suspension of this oxide in water. Addition of two different concentrations of ferric ions to a ferric oxide sample allowed us to show the importance of the ratio $[Fe^{3+}]_{diss}/[Fe_2O_3]$. Apart from this ratio, several other parameters are at the origin of the distinct effects of various ferric oxide samples, among which the crystallinity is noticeable.

Although the concentrations of oxalic acid, ferric ions and ferric oxide used in these laboratory studies were generally higher than those encountered in natural waters, the curves of Figs. 5 and 6 show that extrapolations to lower concentrations can be made. Consequently, the conclusions drawn here may reasonably be expected to remain valid for environmental conditions.

References

[1] P. Warneck, *Chemistry of the Natural Atmosphere*, Academic, San Diego, CA, 1988, Chap. 7, pp. 278–373.
[2] P.M. Foster, *Atmos. Environ., 3* (1969) 157.
[3] B.C. Faust, M.R. Hoffmann and D.W. Bahnemann, *J. Phys. Chem., 93* (1989) 6371.
[4] P. Behra and L. Sigg, *Nature, 344* (1990) 419.
[5] J. Hoigné, Y. Zuo, M. von Pieckowski, R. Bühler and D. Sedlak, in J. Peeters (ed.), *Air Pollution Research Report Workshop Proc., Joint CEC–EUROTRAC Workshop LACTOZ/HALIPP Working Group, CEC, Brussels, 1993*, pp. 5–10.
[6] S.O. Pehkonen, Y. Erel and M.R. Hoffmann, *Preprints Extended Abstracts, Division of Environmental Chemistry, American Chemical Society, San Francisco, CA, April 1992*, p. 533.
[7] J.H. Kennedy and N. Anderman, *J. Electrochem. Soc., 130* (1983) 848.
[8] J.K. Leland and A.J. Bard, *J. Phys. Chem., 91* (1987) 5076.
[9] C. Kormann, D.W. Bahnemann and M.R. Hoffmann, *J. Photochem. Photobiol. A: Chem., 48* (1989) 161.
[10] (a) B. Sulzberger, in W. Stumm (ed.), *Aquatic Chemical Kinetics*, Wiley, New York, 1990, p. 401; (b) B. Sulzberger, H. Laubscher and G. Karametaxas, in G.R. Helz, R.G. Zepp and D.G. Crosby (eds.), *Aquatic and Surface Photochemistry*, Lewis, Boca Raton, FL, 1994, pp. 53–73, and references cited therein.
[11] B.C. Faust and J. Hoigné, *Atmos. Environ. A, 24* (1990) 79.
[12] R.G. Zepp, B.C. Faust and J. Hoigné, *Environ. Sci. Technol., 26* (1992) 313.
[13] Y. Zuo and J. Hoigné, *Environ. Sci. Technol., 26* (1992) 1014.
[14] B. Zinder, G. Furrer and W. Stumm, *Geochim. Cosmochim. Acta, 50* (1986) 1861.
[15] A. Kayo, T. Yamaguchi and K. Tanabe, *J. Catal., 83* (1983) 99.
[16] J.T. Richardson and R.J. Dubus, *J. Catal., 54* (1978) 207.
[17] M. Andrès, *Thèse*, Université Lyon I, 1984, p. 66.
[18] J.-M. Herrmann, J. Disdier and P. Pichat, *J. Chem. Soc., Faraday Trans. 1, 77* (1981) 2815.
[19] J.-M. Herrmann, J. Disdier and P. Pichat, *Chem. Phys. Lett., 118* (1984) 618.
[20] H. Courbon, J. Disdier, J.-M. Herrmann, P. Pichat and J.A. Navio, *Catal. Lett., 20* (1993) 251.
[21] J.H. Bascendale and N.K. Bridge, *J. Phys. Chem., 59* (1955) 783.
[22] M. Hino and K. Arata, *Chem. Lett.*, (1979) 477; *J. Chem. Soc., Chem. Commun.*, (1979) 1148.